Brain and Mind **4:** 51–65, 2003.

Growth Functions in Dendritic Outgrowth

JAAP VAN PELT and HARRY B. M. UYLINGS
Graduate School Neurosciences Amsterdam, Netherlands Institute for Brain Research, Meibergdreef 33, 1105 AZ Amsterdam, The Netherlands, e-mails: j.van.pelt@nih.knaw.nl and h.uylings@nih.knaw.nl

(Received: 15 September 2002; in final form: 5 February 2003)

Abstract. The temporal profile of dendritic branching in developing neurons is an interplay between the proliferating number of branching sites and the branching rates at these individual sites. The eventual metrical structure of dendritic arborizations is the outcome of joint processes of branching and elongation of outgrowing neurites. Dendritic growth models have shown to be powerful tools for quantitatively studying the rules of outgrowth, aiming at reproducing the shape characteristics in observed dendritic arborizations. Recent model studies, focusing on the branching process, have predicted strongly decreasing branching rates during dendritic outgrowth. The implications of these findings for the metrical development of outgrowing dendrites will be discussed.

Key words: branching, dendritic length, elongation, growth cones, growth model.

1. Introduction

The diversity and complexity of neuronal shapes is still poorly understood both from a morphological and functional point of view. This may seem surprising in view of the principal role neurons play in information processing in the nervous system but it essentially illustrates that neuroscience is still at the beginning in unraveling the structure–function relationships within neurons (see for a review Stuart *et al.*, 1999). Progress is stimulated by the availability of computational tools for generating dendrites with realistic morphological variations (e.g., Ascoli, 1999; Ascoli and Krichmar, 2000; Van Pelt *et al.*, 2001; Van Ooyen, 2003) and for calculating the electrical behavior using neural simulators (see reviews in Segev *et al.*, 1995; Koch and Segev, 1998; Poznanski, 1999; De Schutter and Cannon, 2001). These tools now make possible systematic studies of the implications of neuronal morphology on firing patterns, showing for instance that firing rates correlate with dendritic extent (Mainen and Sejnowski, 1996), and that firing patterns correlate with dendritic topology (Duijnhouwer *et al.*, 2001; Van Ooyen *et al.*, 2002). Further development of these tools will stimulate more detailed exploration of the role of dendritic morphology in neuronal signal (and information) processing.

One of the approaches in dendritic modeling is based on developmental principles, aiming at finding rules of neurite elongation and branching that result in dendrites with realistic morphologies (e.g., Van Pelt *et al.*, 2001). Neurons attain their highly branched shapes through a developmental process of neurite elongation and branching. This process is mediated by growth cones, specialized structures at the terminal tips of outgrowing neurites. Growth cones are highly motile structures, which integrate local environmental and intracellular

signals and respond with branching through splitting of the growth cone, and elongation through the polymerization of the microtubular cytoskeleton (e.g., Black, 1994; Kater *et al.*, 1994; Kater and Rehder, 1995; Letourneau *et al.*, 1994). The morphological differentiation between cell types and the diversity between neurons of the same type thus must find their origin in these intracellular and environmental details (e.g., Acebes and Ferrus, 2000). Basic to the outgrowth process is the formation of the dendritic cytoskeleton requiring production, transport, and polymerization of cytoskeletal elements such as tubulin. The dendritic outgrowth process is influenced by complex intracellular regulatory genetic and molecular signaling pathways (e.g., Song and Poo, 2001), electrical activity (e.g., Cline, 1999; Ramakers *et al.*, 1998, 2001; Zhang and Poo, 2001), and a variety of extracellular molecules influencing the behavior of the growth cone (e.g., McAllister, 2002; Whitford *et al.*, 2002).

An interesting question is whether and how the dendritic outgrowth process is subjected to basic constraints that set a limit to the modulatory responsiveness. For instance, one may expect a direct relation between the production rate of cytoskeletal elements and the total length increase of the dendrite. Branching of growth cones implicates an increasing number of sites of branching and elongation in the growing dendrite. Unrestricted proliferation may seem not likely and one may expect that it is under control of rate-limiting and homeostatic mechanisms. Earlier model studies of microtubule polymerization (neurite elongation) in relation to tubulin production and transport demonstrated how limited supply conditions may lead to competition between growth cones for tubulin, resulting in alternating advance and immobilization (Van Ooyen *et al.*, 2001). Empirical evidence for such competitive behavior was subsequently obtained from time-lapse studies of outgrowing neurons in tissue culture by Ramakers (see Da Costa *et al.*, 2002).

A quantitative description of the development of dendritic shape is essential for studying the question how dendritic shape can be understood as an emergent property of the dynamic behavior of growth cones. The complexity of the developmental process requires an integrated computational modeling approach with experimental data on dendritic development to address these issues.

Earlier studies have already shown that (i) topological variation between dendritic trees finds its origin in the varying sequences of branching of the different growth cones and their positions in the tree (e.g., Dityatev *et al.*, 1995; Van Pelt and Uylings, 1999); (ii) the rate of branching depends on the momentary number of growth cones (Van Pelt *et al.*, 1997); and (iii) the rate of branching depends on a time-dependent baseline component (Van Pelt and Uylings, 2002). In this last study it was shown quantitatively how the rate of increase in the number of terminal segments relates to the branching rates of individual growth cones. Application to experimental data from rat cortical multipolar nonpyramidal neurons showed that the baseline branching rate is a rapidly decreasing function of time (approximated by an exponential function) and made explicit how the branching rate of individual growth cones depends on their momentary number in the growing dendrite.

The segment length structure in a dendrite and its total length is the outcome of the joint processes of neurite elongation and branching. Their statistical properties can thus only be understood quantitatively when these two processes are considered simultaneously. In this paper it is shown how the temporal increase in total dendritic length during dendritic

outgrowth relates to the branching process. The mathematical formalism is applied in the analysis of experimental data on the increase of total dendritic length in rat cortical multipolar nonpyramidal neurons. It is shown that the dendritic length growth is well approximated by the model when it is assumed that neurite elongation rates decrease with increasing number of growth cones.

These model-based approaches in analyzing the geometrical development of dendritic branching patterns are essential for quantitative descriptions and have shown to reveal characteristic details, relations, and constraints of the developmental process.

2. Growth of Dendritic Branching Patterns

Dendritic outgrowth will be modeled as a process of elongation and branching of terminal segments. During the biological process of dendritic outgrowth, the dynamic behavior of growth cones includes actions of forward migration and also of retraction or complete disappearance. At a sufficient large timescale the net outcome of these forward and backward movements will nevertheless be observed as a growing dendrite with increasing length and number of branches, as is schematically illustrated in Figure 1.

2.1. DENDRITIC BRANCHING PROCESS

In modeling dendritic branching it will be considered as a stochastic process, with branching events occurring randomly in time. The mean branching probability of a terminal segment $\bar{p}(t)$ is assumed to consist of a (time-dependent) baseline component, and a (competition) component dependent on the momentary number of terminal segments

$$\bar{p}(t) = D(t)\bar{n}(t)^{-E} \tag{1}$$

with $\bar{n}(t)$ the mean number of terminal segments in dendritic trees at time t, $D(t)$ a baseline branching rate function and E a competition parameter (Van Pelt and Uylings, 2002). In

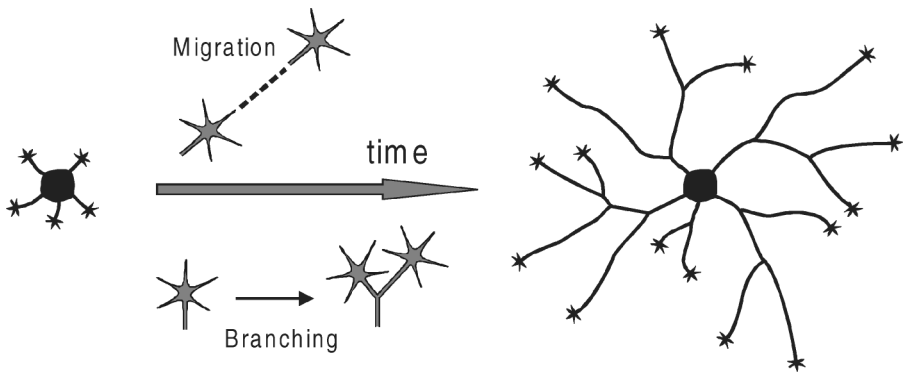

Figure 1. Schematic illustration of the branching and elongation process mediated by growth cones. Initial protrusions from the cell body develop into mature dendritic trees through a process of growth cone elongation and branching.

the following we will discard the bar in $\bar{n}(t)$ and use $n(t)$ with the same meaning. The rate of increase of the number of terminal segments is then given by

$$\frac{dn(t)}{dt} = D(t)n(t)^{1-E} \tag{2}$$

with the general solution for the function $n(t)$ given by

$$n(t) = [1 + E\,B(t)]^{1/E} \text{ for } E > 0, \quad \text{and} \quad n(t) = e^{B(t)} \text{ for } E = 0 \tag{3}$$

with $B(t)$defined by the time integral of function $D(t)$

$$B(t) = \int_0^t D(s)\ ds. \tag{4}$$

The function $B(t)$ can be interpreted as the expected number of branching events at a single terminal segment over a period [0–t]. Equation (3) shows how the expected number of terminal segments at time t depends on parameter E and on $B(t)$, while Eq. (3) can also be rewritten as

$$B(t) = \frac{n^E(t) - 1}{E} \quad \text{for } E > 0, \quad \text{and } B(t) = \log_e(n(t)) \text{ for } E = 0. \tag{5}$$

2.1.1. *Constant Baseline Branching Rate*

If the baseline branching rate is constant during development, $D(t) = D_c$, then $B(t) = D_c t$ and the growth function $n(t)$ becomes

$$n(t|D_c) = [1 + E\,D_c t]^{1/E} \text{ for } E > 0. \tag{6}$$

and

$$n(t|D_c) = e^{D_c t} \text{ for } E = 0. \tag{7}$$

This last case, $E = 0$, when the mean branching probability of a terminal segment is constant, $\bar{p}(t) = D_c$, independent of the total number of terminal segments, thus results in an exponential increase in the number of terminal segments. For $E = 1$, the branching probability of a terminal segment becomes $\bar{p}(t) = D_c/n(t)$, inversely proportional to the number of terminal segments, and resulting in a linear increase of the number of terminal segments

$$n(t|D_c; E = 1) = 1 + D_c t. \tag{8}$$

The influence of the competition parameter E on the temporal increase in the number of terminal segments is illustrated in Figure 2A, with an exponential increase in the case of unrestricted branching ($E = 0$), a linear increase when the branching probability is fully corrected for the increasing number of terminal segments ($E = 1$), and an intermediate course for $E = 0.2$. In all these cases, branching continues with an ongoing increase in the number of terminal segments. Dendritic branching, however, terminates after its developmental period, making the assumption of a constant baseline branching rate not realistic.

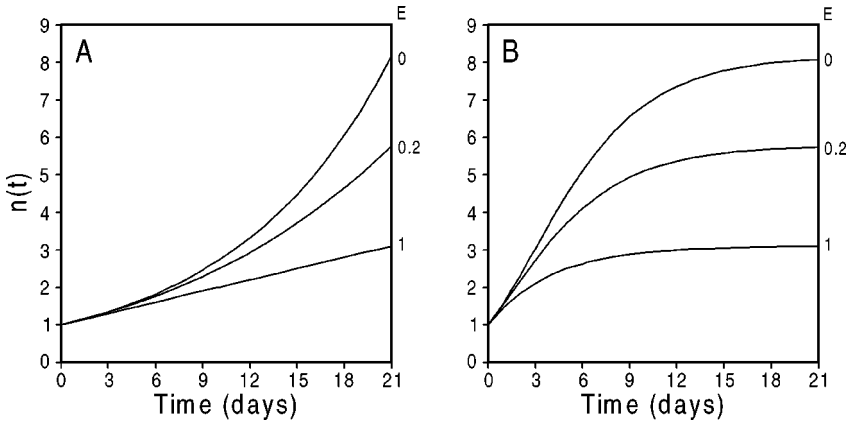

Figure 2. Increase in the number of terminal segments $n(t)$ for (A) a constant value of the baseline branching rate function $D_c = 0.1$ (and thus with $B(21) = 2.1$), and for (B) an exponential baseline branching rate function $D(t) = ce^{-t/\tau}$, with $B_\infty = 2.1$, $\tau = 4$ day, and $c = B_\infty/\tau = 0.525$. Each panel includes growth curves for three values of the competition parameter E , i.e., E= 0, 0.2, and 1, respectively.

2.1.2. *Exponential Baseline Branching Rate Function*

For the termination of the branching process we need therefore to assume that the baseline branching rate goes to zero at the end of the branching process. It was shown in a previous study (Van Pelt and Uylings, 2002) that an exponential decreasing baseline branching rate function resulted in realistic functions for the increasing number of terminal segments, with a stabilization at the end of the branching process.
Thus, assuming

$$D(t) = ce^{-t/\tau} \tag{9}$$

we obtain for the function $B(t)$

$$B(t) = \int_0^t D(s)\, ds = \int_0^t ce^{-s/\tau}\, ds = c\tau(1 - e^{-t/\tau}), \tag{10}$$

which, given the asymptotic value $B_\infty = B(\infty) = c\tau$, can also be written as

$$B(t) = B_\infty(1 - e^{-t/\tau}).$$

Inserting this expression in Eq. (3) we obtain for the growth function $n(t)$,

$$n(t|D(t) = ce^{-t/\tau}) = [1 + E\,B(t)]^{1/E} = [1 + E\,B_\infty(1 - e^{-t/\tau})]^{1/E} \tag{11}$$

for $E > 0$, and

$$n(t|D(t) = ce^{-t/\tau}) = e^{B(t)} = e^{B_\infty(1-e^{t/\tau})} \text{ for } E = 0.$$

For these growth functions, the number of terminal segments initially rapidly increases but finally stabilizes at asymptotic values of

$$n_\infty = n(\infty|D(t) = ce^{-t/\tau}) = [1 + E\,B_\infty]^{1/E} \quad \text{or} \quad E\,B_\infty = n_\infty^E - 1$$
$$\text{for} \quad E > 0, \quad \text{and} \quad n_\infty = e^{B_\infty} \quad \text{or} \quad B_\infty = \log_e(n_\infty) \quad \text{for} \quad E = 0. \tag{12}$$

For the case of $E = 1$, we obtain $n_\infty = 1 + B_\infty$. Because under this condition the branching probability of a terminal segment is corrected for the total number of terminal segments, the number of expected branching events now equals the number expected for a single segment under noncompetitive conditions. Note, that each branching event let the number of terminal segments increase with one, additional to the initial segment at the start of branching. With the expressions (12) for n_∞ we can rewrite Eqs. (11) as

$$n(t) = n_\infty\left[1 - \left(1 - n_\infty^{-E}\right)e^{-t/\tau}\right]^{1/E} \quad \text{for} \quad E > 0 \quad \text{and} \quad n(t) = n_\infty^{1-e^{-t/\tau}} \quad \text{for} \quad E = 0. \quad (13)$$

These equations more explicitly show how the number of terminal segments increases towards its asymptotic value n_∞. Additionally, they may be helpful in finding best estimates for the parameters E and τ, when the value n_∞ can already be estimated from mature dendritic trees. The asymptotic shape of these growth functions is illustrated in Figure 2B for three values of the competition parameter E. These shapes turn out to reproduce observed dendritic growth patterns very well as is demonstrated by Van Pelt and Uylings (2002) for dendrites of rat cortical multipolar nonpyramidal neurons, and also is illustrated in Figure 5A.

2.1.3. *Terminal Segment Number Distributions*

Under stochastic growth rules, trees experience varying number of branching events during their outgrowth, resulting in a distribution for the terminal segment number of individual trees at a particular point in time. The mean of this distribution is given by the expressions for $n(t)$ as derived above and in their dependence on the competition parameter E. The standard deviation could not be derived as a closed analytical expression but had to be obtained using recurrent relations as has been shown in Van Pelt *et al.* (1997, 2002). These studies showed how the standard deviation depended on the competition parameter E, and also demonstrated how this parameter could be estimated using data on mean and standard deviation of the observed terminal segment number distributions.

The description of the branching process now provides an appropriate basis for including elongation of neurites into the growth model and studying the length increase of the outgrowing dendrites.

2.2. DENDRITIC ELONGATION PROCESS

When the individual terminal segments elongate with a mean rate $v(t)$, the total length of the tree $L(t)$ increases with a rate given by

$$\frac{dL(t)}{dt} = n(t)v(t). \quad (14)$$

The total length of the growing dendrite at time t can be obtained by taking the time integral

$$L(t) = \int_o^t n(s)v(s)\, ds, \quad (15)$$

when the initial length of the dendrite at time $t = 0$ is taken to be zero. Inserting the expression for the function $n(t)$ (Eq. (11)), and thus assuming an exponential decreasing

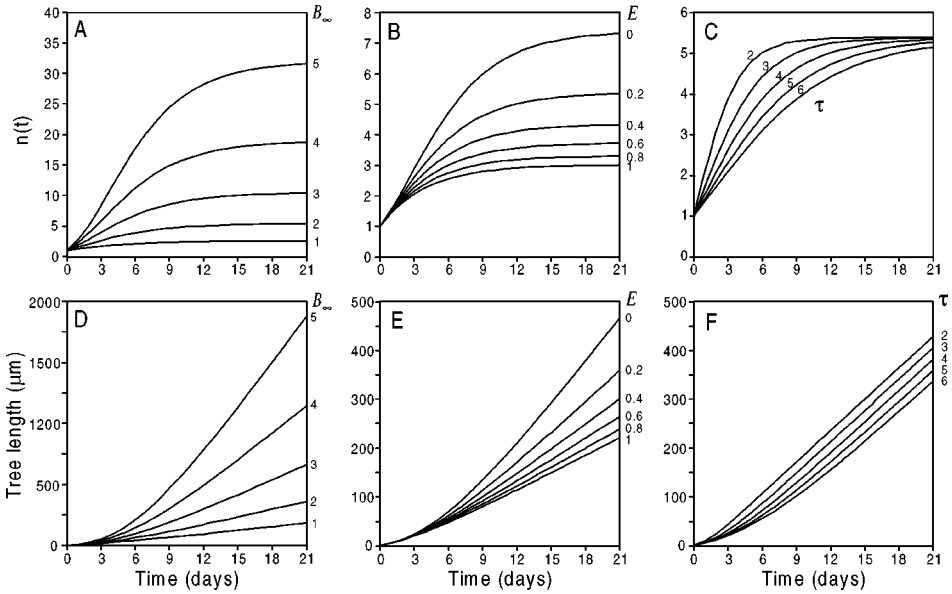

Figure 3. Growth curves for (top row) the number of terminal segments $n(t)$, and (bottom row) for the total length of the trees $L(t)$. The curves have been calculated for a branching process with parameter values $E = 0.2$ and $\tau = 4$ day (left column), $B_\infty = 2$ and $\tau = 4$ day (middle column), and $B_\infty = 2$ and $E = 0.2$ (right column). The growth curves for the total tree length have been obtained assuming a constant elongation rate of $v_c = 4\mu$m/day.

baseline branching rate function, results in

$$L(t) = \int_o^t n(s)v(s)\,ds = \int_0^t [1 + EB_\infty(1 - e^{-s/\tau})]^{1/E} v(s)\,ds \quad \text{for} \quad E > 0,$$

$$\text{and} \quad L(t) = \int_o^t n(s)v(s)\,ds = \int_0^t e^{B_\infty(1-e^{s/\tau})} v(s)\,ds \quad \text{for } E = 0. \tag{16}$$

2.2.1. *Tree-Length Growth Functions With Constant Neurite Elongation Rates*

When the elongation rate is constant, $v(t) = v_c$, the rate of increase of total tree length becomes proportional to the momentary number of elongating neurites $dL(t)/dt = v_c n(t)$, and function $L(t)$ becomes

$$L(t|v_c) = \int_o^t v_c n(s)\,ds = v_c \int_0^t n(s)\,ds. \tag{17}$$

The increase in total tree length $L(t)$ is illustrated in Figure 3 for several combinations of the parameters of the branching process. All these examples show that the length growth functions have increasing derivatives (increasing growth rates) during the branching process, when the number of terminal segments is increasing. When the branching process terminates, the number of terminal segments does not increase anymore, while total tree length further increases with constant rates (constant derivatives).

2.2.2. *Tree-Length Growth Functions With Degree-Dependent Neurite Elongation Rates*

A primary requirement for neurite elongation is the polymerization of the microtubular cytoskeleton. In a branched structure the tubulin molecules, produced in the cell body, need to be transported to and divided among all the present growth cones as their major sites for polymerization into the microtubules. It may therefore be unlikely that the neurite elongation rate remains constant when the number of growth cones increases during the branching process. To be able to account for such effects we assume that the elongation rate depends on the momentary number of growth cones, via

$$v(t) = v_0 n(t)^{-F} \tag{18}$$

with parameter F modulating the strength of this dependency. Inserting Eqs. (11) and (18) into Eq. (15) we obtain for the tree-length growth function

$$L(t) = \int_0^t n(s) v_0 n(s)^{-F} ds = v_0 \int_0^t [1 + E B_\infty (1 - e^{-s/\tau})]^{(1-F)/E} ds. \tag{19}$$

For a constant neurite elongation rate ($F = 0$), independent of the momentary number of elongating terminal neurites, the growth function becomes,

$$L(t|F = 0) = v_0 \int_0^t n(t)\ ds, \tag{20}$$

which is the condition as described in the previous paragraph. Then, the length of the tree increases with increasing rate when the number of terminal segments increases, and becomes constant when branching is terminating, as is shown in Figure 4B.

A value of one for the parameter F indicates that the neurite elongation rate is inversely proportional to the momentary number of elongating terminal neurites, resulting in the length growth function

$$L(t|F = 1) = v_0 \int_o^t ds = v_0 t. \tag{21}$$

While the elongation rate of individual segments decreases with increasing number of terminal segments, the increase in total length remains constant, independent of the number of terminal segments. The constant increase in total tree-length is illustrated in Figure 4B by the linear curve for $F = 1$. This condition reflects a situation when a constant production of cytoskeletal molecules is distributed among an increasing number of polymerization sites.

2.2.3. *Initial Length and Time of Onset of Branching*

If the branching process starts at time t_0, and the initial neurite had already an initial length L_0, Eq. (19) is generalized into the tree-length growth function

$$L(t) = L_0 + v_0 \int_{t_0}^t [1 + E B_\infty (1 - e^{-(s-t_0)/\tau})]^{(1-F)/E}\ ds. \tag{22}$$

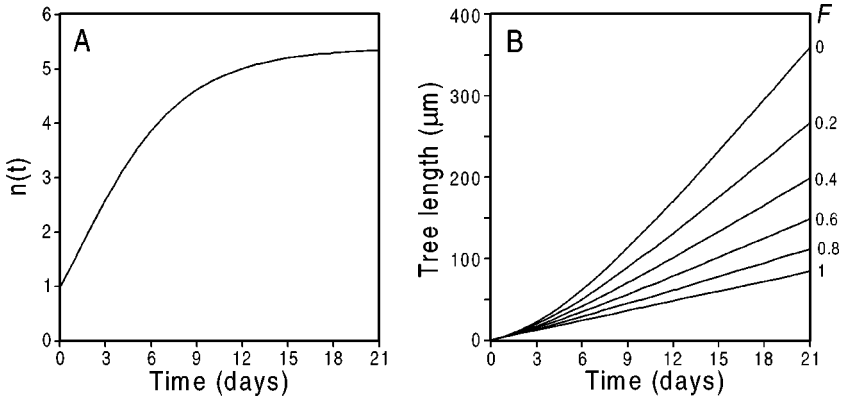

Figure 4. Growth curves for (A) the number of terminal segments $n(t)$, and (B) the total length of the trees $L(t)$. The curves have been calculated for a branching process with parameter values $B_\infty = 2$, $E = 0.2$and $\tau = 4$ day. The growth curves for the total tree-length in (B) have been obtained assuming an elongation rate dependent on the number of terminal segments, $v(t) = v_0 n(t)^{-F}$, for different values of the parameter F.

2.2.4. *Asymptotic Elongation Rates*

When the number of terminal segments reaches its asymptotic value n_∞, the elongation rate will stabilize at $v_\infty = v_0 n_\infty^{-F}$, which, using Eq. (12), can be written as

$$v_\infty = v_0 n_\infty^{-F} = v_0[1 + E\,B_\infty]^{-F/E} \tag{23}$$

3. Application to the Growth of Rat Layer IV Multipolar Nonpyramidal Dendritic Trees (Parnavelas and Uylings, 1980; Uylings *et al.*, 1980)

The increase in the number of terminal segments during branching has been studied in Van Pelt and Uylings (2002). In this paper four different approaches have been discussed to find estimates for the terminal segment number growth functions in combination with an estimate for the baseline branching rate function. These approaches were illustrated using a data set of the development of rat layer IV multipolar nonpyramidal neurons obtained from the studies of Parnavelas and Uylings (1980) and Uylings *et al.* (1980), and summarized in Table I.

Following approach I in this study (Van Pelt and Uylings, 2002), assuming branching to start at $t_0 = 1$ day postnatal, and assuming an exponential baseline branching rate function, it was found that the growth of the number of terminal segments was best described by the terminal segment number growth function $n_{\text{est}}(t) = 2.96[1 - 0.071\,e^{-t/3.7}]^{19.6}$, or after rewriting $n_{\text{est}}(t) = 2.96[1 - 0.054\,e^{-(t-1)/3.7}]^{19.6}$ and which was based on the baseline branching rate function $D(t) = 0.304\,e^{-(t-1)/3.7}$. These results were obtained for a competition parameter $E = 0.051$, and a decay constant $\tau = 3.7$ days, with $n_\infty = 2.96$ and $B_\infty = 1.124$. Both the baseline branching rate function and the optimized terminal segment number growth function are displayed in Figure 5A, which also includes the original data points for the mean and SD values of the observed number of terminal segments.

Table I. Observed data and model results for the mean and SD of the distributions of the terminal segment number, and of the total length of dendritic trees of rat layer IV multipolar nonpyramidal neurons at several development stages (4, 6, 8, 10, 12, 14, 16, 18, 20, 24, and 90 days)

		Number of Terminal Segments Per Tree		Total Length (μm)	
Age (days)	Number of Trees	Mean	SD	Mean	SD
4	37	1.76	0.95	40.2	28.0
6	113	2.08	1.62	55.7	60.1
8	121	2.66	2.22	75.6	81.5
10	121	2.92	2.01	92.9	79.7
12	204	2.95	2.42	130.8	137.5
14	175	2.99	2.68	130.5	138.0
16	238	3.29	2.51	172.7	175.0
18	212	2.75	1.99	170.1	182.8
20	219	2.78	2.11	165.0	173.9
24	172	2.79	1.93	163.2	155.8
90	226	2.99	2.31	214.4	191.9

Note. The experimental data originate from morphometrical studies of the growth of nonpyramidal neurons in the visual cortex of the rat (Parnavelas and Uylings, 1980; Uylings *et al.*, 1980). The data from the coronal sections have been reanalysed in the present study in order to obtain the number of terminal segments and total length of individual dendrites at the different developmental stages.

With the estimate for the terminal segment number growth function, the length growth function was subsequently obtained by optimizing the parameters L_0, v_0 and F in Eq. (22) to the experimental data set for the dendritic tree-lengths at the different time points during their outgrowth (Table I), the results of which are shown in Figure 5B–D. Assuming a fixed value for the initial length $L_0 = 10$ μm (taken from the mean intermediate segment length at postnatal day 4 in this data set), this resulted in an estimate for the elongation rate function $v(t) = v_0 n(t)^{-F}$ with $v_0 = 8.1$ μm/day and $F = 0.74$ (Figure 5B). For illustration the optimization results for fixed values of $F = 0$ (Figure 5C) and $F = 1$ (Figure 5D) are also included. Table II lists the optimized values for the parameter sets as well as the obtained value for the chi square. For the optimization, procedure MRQMIN was used from Press *et al.* (1992).

The differences in the quality of the fits to this data set appear to be relatively small, but especially visible in the shape of the length growth function in the early days of development (Figure 5B–D). A constant elongation rate ($F = 0$) resulted in an estimated value for the initial length $L_0 = 22.0$ μm. This value seems unrealistically large in comparison with the mean intermediate segment length of 10 μm in these dendrites (see also Uylings *et al.*, 1994) in the first days of development. Under the condition $F = 1$, a linear growth curve is obtained (Figure 5D, see also Eq. (21)), resulting in a lesser optimal fit. A value for the initial length of $L_0 = 10$ μm resulted in an optimized value of $F = 0.74$ in combination with an elongation rate parameter of $v_0 = 8.2$ μm/day (Figure 5B). These outcomes demonstrate that a dependence of the elongation rate on the number of terminal segments becomes

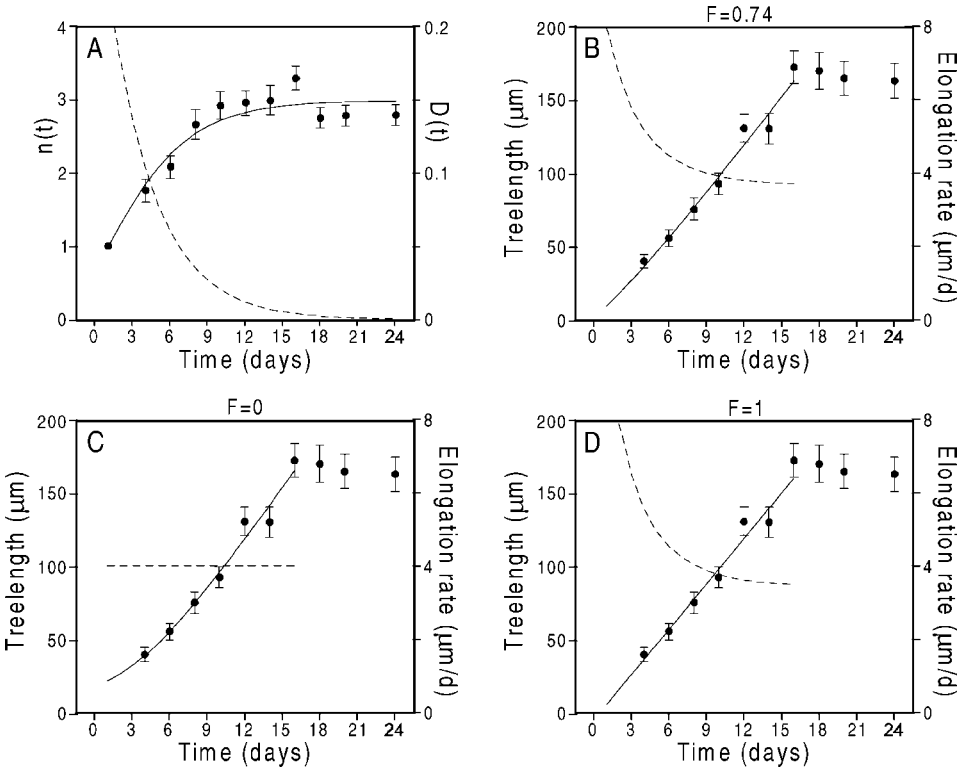

Figure 5. (A) Mean and SD (data points) of the number of terminal segments of dendrites of rat cortical multipolar nonpyramidal cells at several time points during development (see Table I). The terminal segment number growth function (solid line) $n_{\text{est}}(t) = n_\infty[1 - (1 - n_\infty^{-E})e^{-(t-t_0)/\tau}]^{1/E}$ is obtained for $t_0 = 1$ day, $\tau = 3.7$ day, $n_\infty = 2.96$, $E = 0.051$, and assuming an exponential baseline branching rate function (dashed line) $D(t) = ce^{-(t-t_0)/\tau}$, with $B_\infty = 1.12$ and $c = B_\infty/\tau = 0.304$. (B–D) Mean and SEM (data points) of the total length of dendritic trees of rat cortical multipolar nonpyramidal cells at several time points during development (see Table I). The tree-length growth functions (solid lines) have been obtained by fitting Eq. (22) to the data points with fixed values of $L_0 = 10$ μm (panel B), $F = 0$ (panel C), and $F = 1$ (panel D), and optimized values as given in Table II, and using the above given estimated function $n_{\text{est}}(t)$. The corresponding elongation rate functions $v(t) = v_0 n(t)^{-F}$ are shown as dashed lines in panels (B–D).

Table II. Combinations of values for the elongation parameters L_0, v_0, and F, obtained by fitting Eq. (22) to the experimental data in Table I

L_0 (μm)	v_0 (μm/day)	F	Chi Square	Asymptotic Elongation Rate (μm/day)
22.0	4.0	0[a]	3.4	4.0
6.4	10.3	1[a]	4.7	3.5
10[a]	8.2	0.74	4.3	3.7

Note. Parameters with predefined values are indicated with *. The 4th column lists the chi-square values when SEM values were used as weight factors in the fit procedure (Press *et al.*, 1992). The 5th column lists the values for the expected elongation rate when the number of terminal segments has reached its asymptotic value of $n_\infty = 2.96$, using Eq. (23) $v_\infty = v_0 n_\infty^{-F}$, and the values for v_0 and F from the 2nd and 3rd column, respectively.

expressed in subtle changes in the shape of the length growth curve. Additionally they give support to the hypothesized effect of the terminal segment number on the elongation rates.

When the number of terminal segments approaches its asymptotic value of $n_\infty = 2.96$, also the length growth curves for $F \neq 1$ adopt a more linear pattern. Simultaneously, elongation rates go down for $F > 0$, and, as the dashed curves in Figure 5B and D show, converge to a value quite close to the constant elongation rate of $v_0 = 4$ μm/day for $F = 0$ in Figure 5C. The estimated elongation rates at day 16 (5th column in Table II), calculated using the Eq. (23) $v_\infty = v_0 n_\infty^{-F}$, indeed fall in a small range of 3.5–4.0 μm/day, and thus appear to be less sensitive to the individual values for the different parameter. After day 16, dendritic length promptly stabilizes, indicating that neurite elongation rates abruptly drops down to zero.

4. Discussion

A mathematical framework has been presented for the quantitative description of the growth of dendritic branching patterns. Assuming a stochastic process, the behavior of growth cones has been described in terms of a branching probability and an elongation rate per unit of time. The increase in the number of terminal segments is the outcome of the branching process. The increase in total dendritic length, however, is the joint outcome of both the branching and elongation process of all its (increasing number of) terminal segments. In this study it is illustrated how total dendritic length increases under different assumptions of the branching probability and elongation rate in their dependence on the increasing number of terminal segments. The mathematical framework allows the analysis of experimental data sets of dendritic branching patterns at different time points in terms of branching and elongation rates of their growth cones.

The branching probability was taken to depend on a baseline branching rate component and a (competition) component dependent on the momentary number of terminal segments. It was already shown in earlier studies that the baseline branching rate component must be a rapidly decreasing function of time in order to obtain an asymptotic growth function for the number of terminal segments. The competition component was derived in earlier studies from the relation between mean and standard deviation of the terminal segment number distributions (Van Pelt *et al.*, 1997). In the present study the elongation rate was also made dependent on the momentary number of terminals segments. Without competition, the elongation rate remains constant independent of the number of growth cones. Then, total dendritic length increases with increasing rate when the number of growth cones increases, and increases with a constant rate when the number of growth cones stabilizes. With strong competition, i.e., when elongation rate is inversely proportional to the number of terminal segments, total dendritic length increases linearly in time, independent of the branching process. The shape of the actual growth curve for total dendritic length thus provides information about possible competitive effects on elongation during dendritic outgrowth.

The dendritic growth model has been applied to the outgrowth of rat cortical multipolar nonpyramidal dendritic trees. Empirical data on the branching process has already been analyzed in previous studies. The mean and standard deviation in the number of terminal

segments in the 16-day dendritic trees was used to find an estimate of the branching competition parameter (Van Pelt *et al.*, 2002), while similar data at all the measured time points was used to find an averaged estimation of the competition parameter and an estimate for the time course of the baseline branching rate function (Van Pelt and Uylings, 2002). Using these findings and including empirical data on the growth of total dendritic length, it was possible in the present study to obtain a quantitative description of the joint branching and elongation process. It was shown how a dependence of the elongation rate on the number of terminal segments becomes expressed in typical shape differences in the total length growth functions. Analyzing the present data it was shown that a constant elongation rate resulted in an unrealistic value for the initial length, supporting the hypothesis that elongation rate decreases with increasing number of terminal segments. Using an estimate for the initial length of 10 μm, a good fit was found for an elongation rate parameter of $v_0 = 8.1$ μm/day and an elongation competition parameter of $F = 0.73$. For positive values of F, the estimated elongation rate functions decrease during the first phase of branching when the number of terminal segments rapidly increases, approaching a constant value when the number of terminal segments stabilizes. These values appeared to be quite close to the elongation rate under constant elongation rate conditions. Therefore, a robust estimation could be made for the elongation rate at the end of the branching process at postnatal day 16 of $3.5 < v(16) < 4$ μm/day. At this point in time total length increase abruptly terminates, suggesting elongation rates to drop down rapidly to zero. These abrupt changes indicate that other mechanisms, not included in the dendritic growth model, get control over the elongation rate, for which reason the present analysis has been restricted to the period up to postnatal day 16.

A positive dependence of the elongation rate on the number of terminal segments may indicate a competitive process within the outgrowing dendrite when an increasing number of growth cones compete for cytoskeletal elements, essential for the further polymerization of the cytoskeleton at their outgrowing sites. Computational studies on tubulin production, transport, and microtubule polymerization already showed how limited supply of tubulin could result in competitive behavior of alternating advance and immobilization of growth cones (Van Ooyen *et al.*, 2001). Experimental evidence for such a type of growth cone behavior was subsequently obtained from time-lapse studies of neurite outgrowth in cultured tissue, showing at short timescales alternating and mutually excluding advances and immobility between growth cones in an outgrowing neuron (Da Costa *et al.*, 2002). When one growth cone advances rapidly, others slow down, followed by an advancement of another growth cone suppressing on its turn the advancement of the other growth cones. The competition for cytoskeletal elements may be one of a range of competitive mechanisms in the outgrowing neurons, as has been emphasized in a review on modeling studies on these issues in Van Ooyen (2001), and Van Ooyen and Van Pelt (2002).

The present study is the first one, relating growth functions of total dendritic length and number of terminal segments with elongation and branching rates of the individual growth cones. The mathematical formalism can be applied to any empirical data set for which these growth functions are available, an example as has been given in the present study for the rat cortical multipolar nonpyramidal dendritic trees. Such studies are especially

interesting when the dendrites grow up to a large number of terminal segments, when competitive mechanisms may be expressed even stronger than in the present data set of relatively moderately branched nonpyramidal dendritic trees. Quantitative data on dendritic shapes derives from 2D and 3D dendritic reconstructions using computer controlled dendrite measuring systems (e.g., Uylings *et al.*, 1986; Glaser and Glaser, 1990) or from advanced procedures for the analysis of digital images (e.g., Masseroli *et al.*, 1993; Cesar and Da Costa, 1999).

The experimental data used in this study resulted from 3D reconstructions of Golgi stained rat cortical multipolar nonpyramidal neurons (Parnavelas and Uylings, 1980; Uylings *et al.*, 1980). These data have not been corrected for possible shrinkage of the tissue prior to reconstruction, implicating that the data on segment length and total dendritic length should be used modulo a (unknown) scale factor. This also applies to any information derived from these data, as the expectations on elongation rates, derived in this study.

References

Acebes, A. and Ferrus, A., 2000: Cellular and molecular features of axon collaterals and dendrites, *Trends Neurosci*. **23**, 557–565.

Ascoli, G. A., 1999: Progress and perspectives in computational neuroanatomy. *Anat. Rec.* **257**(6), 195–207.

Ascoli, G. A. and Krichmar, J. L., 2000: L-Neuron: A modeling tool for the efficient generation and parsimonious description of dendritic morphology, *Neurocomputing* **32/33**, 1003–1011.

Black, M. M., 1994: Microtubule transport and assembly cooperate to generate the microtubule array of growing axons, *Prog. Brain Res.* **102**, 61–77.

Cesar R. M., Jr. and Da Costa, F. L., 1999: Dendrogram generation for neural shape analysis, *J. Neurosci. Method*. **93**, 121–131.

Da Costa, F. L., Tadeu Monteiro Manoel, E., Faucereau, F., Chelly, J. , Van Pelt, J. and Ramakers, G. J. A., 2002: A shape analysis framework for neuromorphometry, *Network: Comput. Neural Syst*. **13**, 283–310.

De Schutter, E. and Cannon, R. C. (eds.), 2001: *Computational Neuroscience: Realistic Modeling for Experimentalists*, CRC Press, Boca Raton, FL.

Dityatev, A. E., Chmykhova, N. M., Studer, L., Karamian, O. A., Kozhanov, V. M. and Clamann, H. P., 1995: Comparison of the topology and growth rules of motoneuronal dendrites, *J. Comp. Neurol.* **363,** 505–516.

Duijnhouwer, J., Remme, M. W. H., Van Ooyen, A., and Van Pelt, J., 2001: Influence of dendritic topology on firing patterns in model neurons, *Neurocomputing* **38–40**, 183–189.

Glaser, J. R. and Glaser, E. M., 1990: Neuron imaging with neurolucida—a PC-based system for image combining microscopy, *Comput. Med. Imag. Graphics* **14**, 307–317.

Kater, S. B., Davenport, R. W. and Guthrie, P. B., 1994: Filopodia as detectors of environmental cues: Signal integration through changes in growth cone calcium levels, *Prog. Brain Res.* **102**, 49–60.

Kater, S.B. and Rehder, V., 1995: The sensory-motor role of growth cone filopodia, *Curr. Opin. Neurobiol.* **5**, 68–74.

Koch, C. and Segev, I., 1998: *Methods in Neuronal Modeling: From Ions to Networks*, MIT Press, Cambridge, MA.

Letourneau, P. C., Snow, D. M. and Gomez, T. M., 1994: Growth cone motility: Substratum-bound molecules, cytoplasmic $[Ca^{2+}]$ and Ca^{2+}-regulated proteins, *Prog. Brain Res.* **102**, 35–48.

Mainen, F. Z. and Sejnowski, T. J., 1996: Influence of dendritic structure on firing patterns in model neocortical neurons, *Nature* **382**, 363–366.

Masseroli, M., Bollea, A. and Forloni, G., 1993: Quantitative morphology and shape classification of neurons by computerized image analysis, *Comp. Methods Prog. Biomed.* **41**, 89–99.

Parnavelas, J. G. and Uylings, H. B. M., 1980: The growth of non-pyramidal neurons in the visual cortex of the rat: A morphometric study, *Brain Res*. **193**, 373–382.

Poznanski, R. R. (ed.), 1999: *Modeling in the Neurosciences*, Harwood, Amsterdam.

Press, W. H., Teukolsky, S. A., Vettering, W. T. and Flannery, B. P. (eds.), 1992: *Numerical Recipes in FORTRAN, The Art of Scientific Computing*, 2nd edn., Cambridge University Press, New York.

Ramakers, G. J. A., Avci, B., Van Hulten, P., Van Ooyen, A., Van Pelt, J., Pool, C. W. and Lequin, M. B., 2001: The role of calcium signaling in early axonal and dendritic morphogenesis of rat cerebral cortex neurons under non-stimulated growth conditions, *Dev. Brain Res*. **126**, 163–172.

Ramakers, G. J. A., Winter, J., Hoogland, T. M., Lequin, M. B., Van Hulten, P., Van Pelt, J. and Pool, C. W., 1998: Depolarization stimulates lamellipodia formation and axonal but not dendritic branching in cultured rat cerebral cortex neurons, *Dev. Brain Res*. **108**, 205–216.

Segev, I., Rinzel, J. and Shepherd G. M. (eds.), 1995: *The Theoretical Foundation of Dendritic Function*, MIT Press, Cambridge, MA.

Song. H. J. and Poo, M. M., 2001: The cell biology of neuronal navigation, *Nat. Cell Biol*. **3**, E81–E88.

Stuart, G., Spruston, N. and Hausser M. (eds.), 1999: *Dendrites*, Oxford University Press, Oxford, UK.

Uylings, H. B. M., Parnavelas, J. G., Walg, H. and Veltman, W. A. M., 1980: The morphometry of the branching pattern of developing non-pyramidal neurons in the visual cortex of rats, *Mikroskopie* **37**, 220–224.

Uylings, H. B. M., Ruiz-Marcos, A. and Van Pelt, J., 1986: The metric analysis of three-dimensional dendritic tree patterns: A methodological review, *J. Neurosci. Methods* **18**, 127–151.

Van Ooyen, A., 2001: Competition in the development of nerve connections: A review of models, *Network: Comput. Neural Syst*. **12**, R1-R47.

Van Ooyen, A. (ed.), 2003: *Modeling Neural Development*, MIT Press, Cambridge, MA.

Van Ooyen, A., Duijnhouwer, J., Remme, M. W. H. and Van Pelt, J., 2002: The effect of dendritic topology on firing patterns in model neurons, *Network: Comput. Neural Syst.* **13**, 311–325.

Van Ooyen, A., Graham, B. P. and Ramakers, G. J. A., 2001: Competition for tubulin between growing neurites during development, *Neurocomputing* **38–40**, 73–78.

Van Ooyen, A. and Van Pelt, J., 2002: Competition in neuronal morphogenesis and the development of nerve connections, in G. A. Ascoli (ed.), *Computational Neuroanatomy: Principles and Methods*, Humana Press, Totowa, NJ, pp. 219–244.

Van Pelt, J., Dityatev, E. and Uylings, H. B. M., 1997: Natural variability in the number of dendritic segments: Model-based inferences about branching during neurite outgrowth, *J. Comp. Neurol*. **387**, 325–340.

Van Pelt, J., Graham, B. P. and Uylings, H. B. M., 2003: Formation of dendritic branching patterns, in A. van Ooyen (ed.), *Modeling Neural Development*, MIT Press, Cambridge, MA.

Van Pelt, J. and Uylings, H. B. M., 1999: Natural variability in the geometry of dendritic branching patterns. in R. R. Poznanski (ed.), *Modeling in the Neurosciences—From Ionic Channels to Neural Networks*, Harwood, Amsterdam, pp. 79–108.

Van Pelt, J. and Uylings, H. B. M., 2002: Branching rates and growth functions in the outgrowth of dendritic branching patterns, *Network: Comput. Neural Syst*. **13**, 261–281.

Van Pelt, J., Van Ooyen, A. and Uylings, H. B. M., 2001: Modeling dendritic geometry and the development of nerve connections, in E. De Schutter (ed.), Cannon RC (CD-ROM) *Computational Neuroscience: Realistic modeling for Experimentalist*, Ch. 7, CRC Press, Boca Raton, FL, pp. 179–208.

Whitford, K. L., Marillat, V., Stein, EW., Goodman, C. S., Tessier-Lavigne, M., Chedotal, A. and Ghosh, A., 2002: Regulation of cortical dendrite development by slit-robo interactions, *Neuron* **33**, 47–61.

Zhang, L. I. and Poo, M. M., 2001: Electrical activity an development of neural circuits, *Nat. Neurosci.* **4** (Suppl.), 1207–1214.